



**HAL**  
open science

## Efficient Dechlorination of $\alpha$ -Halocarbonyl and $\alpha$ -Haloallyl Pollutants by Electroreduction on Bismuth

Yao-Yin Lou, Philippe Hapiot, Didier Floner, Florence Fourcade, Abdeltif Amrane, Florence Geneste

► **To cite this version:**

Yao-Yin Lou, Philippe Hapiot, Didier Floner, Florence Fourcade, Abdeltif Amrane, et al.. Efficient Dechlorination of  $\alpha$ -Halocarbonyl and  $\alpha$ -Haloallyl Pollutants by Electroreduction on Bismuth. *Environmental Science and Technology*, 2020, 54 (1), pp.559-567. 10.1021/acs.est.9b05732 . hal-02442229

**HAL Id: hal-02442229**

**<https://univ-rennes.hal.science/hal-02442229v1>**

Submitted on 13 Feb 2020

**HAL** is a multi-disciplinary open access archive for the deposit and dissemination of scientific research documents, whether they are published or not. The documents may come from teaching and research institutions in France or abroad, or from public or private research centers.

L'archive ouverte pluridisciplinaire **HAL**, est destinée au dépôt et à la diffusion de documents scientifiques de niveau recherche, publiés ou non, émanant des établissements d'enseignement et de recherche français ou étrangers, des laboratoires publics ou privés.



## 25 1. INTRODUCTION

26

27 Bismuth is a white-pink brittle metal well-known as an environmentally benign element  
28 obtained at a relatively low cost and for its intrinsic properties such as its high hydrogen  
29 evolution overpotential, its high diamagnetic susceptibility and low thermal conductivity.

30 Owing to the increasing emphasis on greener catalysts, bismuth metal and its oxidation state

31 Bi(III) have been widely studied in the last fifteen years for their catalytic ability.<sup>1-3</sup> Bi(III)

32 catalyzes many essential reactions in organic synthesis as for example oxidation, alkylation,

33 allylation, cycloaddition and etherification. A few reactions involving Bi(0) catalyst have been

34 also described as for example a Reformatsky-type reaction occurring in the presence of BiCl<sub>3</sub>

35 and Al(0)<sup>4</sup> and the selective reduction of  $\alpha,\beta$ -unsaturated esters with the NaBH<sub>4</sub>-BiCl<sub>3</sub> system.<sup>5</sup>

36 Whereas bismuth metal was not active, its generation *in situ* by a reductive agent allowed the

37 reactions to occur. Bi(0) activated by fluoride salts has also shown a high catalytic ability

38 toward the dehalogenation of  $\alpha$ -halocarbonyl compounds.<sup>6</sup>

39 Bismuth metal has been also studied as electrocatalyst material to achieve electrochemical

40 reductions. Thus, the reduction of nitro derivatives on a platinum electrode modified by

41 underpotentially-deposited monolayers of bismuth has been investigated.<sup>7-9</sup> The presence of Bi

42 adatoms on Pt allowed the extension of the potential window and catalysed the four-electron

43 reduction of the nitroaromatic group *via* an electron-transfer mechanism and not by a

44 hydrogenation mechanism as on Pt. Interesting catalytic properties toward the reduction of O<sub>2</sub>

45 and H<sub>2</sub>O<sub>2</sub> have been also observed with electrodes prepared by underpotential deposition of Bi

46 on Au(111) surfaces.<sup>10,11</sup> Although dioxygen reduction occurs *via* a four-electron pathway, the

47 formation of superoxide on the surface after the transfer of one electron suggested a serial

48 mechanism.<sup>12</sup> More recently, bismuth metal has shown interesting catalytic properties for the

49 selective hydrogenation of biomass chemicals such as 5-hydroxymethylfurfural<sup>13-14</sup> and

50 glucose<sup>15</sup> and for the electroreduction of CO<sub>2</sub> toward the formation of formate or carbon  
51 monoxide depending on the nature of the electrolytic medium.<sup>16-19</sup>  
52 Contamination of soil, groundwater and surface water by synthetic halogenated organic  
53 chemicals has resulted in an increasing interest for reductive dehalogenation reactions since it  
54 often rendering them less offensive environmentally. Many metals such as silver,<sup>20-21</sup>  
55 palladium,<sup>22</sup> gold,<sup>23</sup> copper<sup>24-25</sup> and nickel<sup>26</sup> have shown good catalytic activity toward the  
56 electroreduction of chlorinated compounds. However, to our knowledge, bismuth metal has  
57 never been described as catalyst for the electroreduction of chlorinated compounds. In the  
58 course of our study to perform the dehalogenation of chloroacetanilide herbicides by  
59 electrochemical reduction processes,<sup>26-29</sup> we observed that bismuth metal has a high  
60 electrocatalytic activity toward the reduction of alachlor. In this work, the electrocatalytic  
61 behavior of bismuth toward the reductive dechlorination of several chloroacetamide pollutants  
62 was therefore investigated. Its ability to reduce other compounds containing an activated carbon  
63 atom was highlighted. Mechanistic investigations were performed to understand the high  
64 reactivity of bismuth metal toward chloroacetamide compounds.

65

## 66 **2. 2. EXPERIMENTAL SECTION**

67

68 **2.1. Chemical and materials.** Alachlor (2-Chloro-*N*-(2,6-diethylphenyl)-*N*-  
69 (methoxymethyl)acetamide) and dimethenamid (2-Chloro-*N*-(2,4-dimethyl-3-thienyl)-*N*-(2-  
70 methoxy-1-methylethyl)acetamide) were supplied by Sigma-Aldrich, USA, and  
71 trichloroacetamide (2,2,2-trichloroacetamide) and allyl chloride (3-Chloroprop-1-ene) from  
72 Acros Organics, Belgium. Dichloroacetamide (2,2-dichloroacetamide) was obtained from  
73 Merck KGaA, USA and chloroacetamide (2-chloroacetamide) was provided by Alfa Aesar,  
74 USA. Pretilachlor (2-Chloro-2',6'-diethyl-*N*-(2-propoxyethyl)acetanilide) was bought from

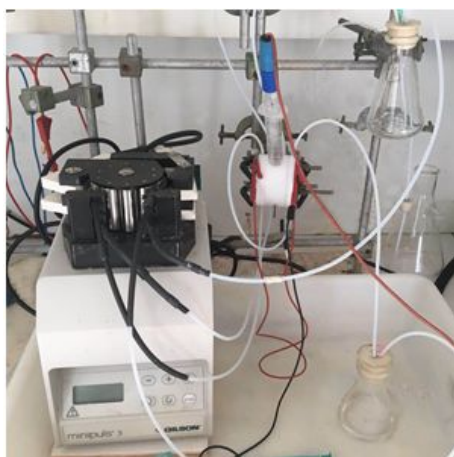
75 TCL, Japan and trichloroacetic acid and chloroacetic acid from Janssen Chimica, Belgium. The  
76 preparation and main characterizations of bismuth modified graphite felt has been previously  
77 reported.<sup>30</sup> The material has a specific surface area of  $0.40 \pm 0.03 \text{ m}^2 \text{ g}^{-1}$  and a bulk density of  
78  $0.181 \pm 0.007 \text{ g cm}^{-3}$ , corresponding to a Bi loading of  $1.7 \text{ mg cm}^{-2}$  and a thickness for the Bi  
79 layer from 0.5 to  $1 \mu\text{m}$ .

80

81 **2.2. Electrochemical analysis.** Cyclic and linear voltammetry analyses were carried out using  
82 a VersaSTAT3 AMETEK Model (Princeton Applied Research) potentiostat/galvanostat. A  
83 bismuth electrode ( $1.77 \text{ mm}^2$ ) prepared by electrodeposition of bismuth on a copper electrode  
84 (disk of 1 mm diameter) (in  $1 \text{ mol L}^{-1} \text{ Bi}_2\text{O}_3$  with 1.1 equivalents of 2,2-Bis(hydroxymethyl)-  
85 2,2',2'-nitrilotriethanol at pH 14 for 30 min, 1 mA) or a glassy carbon electrode ( $0.78 \text{ mm}^2$ ), a  
86 platinum plate auxiliary electrode, and a reference electrode (Mercury-mercurous sulfate –  
87 MSE) were used in a standard three-electrode configuration. The working electrodes were  
88 carefully polished before use and an electroreduction in the studied electrolyte medium at  $-2$   
89  $V_{\text{MSE}}$  for 10s was performed on the bismuth electrode before each analysis.

90 **2.3. Flow electroreduction of chlorinated compounds.** The electrochemical reduction of  
91 chlorinated compounds was performed in a home-made flow cell (Figure 1).

92



93

94 **Figure 1.** Home-made electrochemical flow cell

95

96 To ensure a good homogeneity of the potential distribution in the three dimensional working  
97 electrodes, the bismuth modified graphite felt electrode was located between two  
98 interconnected DSA counter-electrodes (dimensionally stable anodes, AC-2004, supplied by  
99 ECS International Electro Chemical Services, France).<sup>31</sup> The compartments were separated by  
100 cationic exchange membranes (Nafion™ 417 membrane, France) and the reference electrode  
101 (Mercury-mercurous sulfate – MSE) was positioned in the middle of the working electrode (10  
102 mm diameter and 1.7 mm thickness). The solution percolated the porous electrode using a  
103 Gilson minipuls 3 peristaltic pump (Middleton, WI, USA).

104 **2.4. Analytical chromatography.** The concentration of chloride ions (diluted four times)  
105 before and after electrolysis was determined using DIONEX DX120 ion chromatography  
106 equipped with a conductivity detector and a DIONEX AS19 (4 × 250 mm) ion-exclusion  
107 column. The sample was eluted with potassium hydroxide at a flow rate of 1 mL min<sup>-1</sup>. The  
108 detection was carried out by conductivity with a Self-Regenerating Suppressor (SRS).

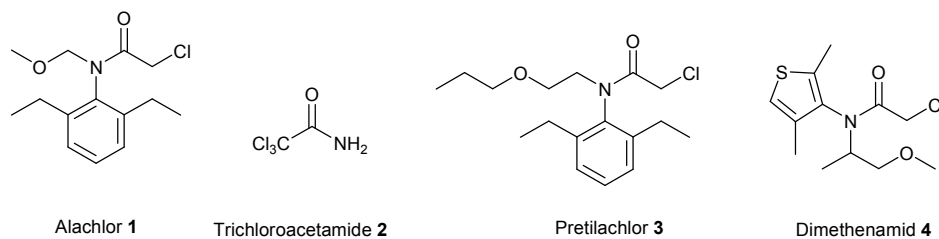
The concentration of alachlor and deschloralachlor were determined using a Waters 996 High  
Performance Liquid Chromatography (HPLC) system equipped with a Waters 996 PDA  
(Photodiode Array Detector) and a Waters 600 LCD Pump. The separation was achieved on a  
Waters C-18 (5 μm; 4.6 × 250 mm) reversed-phase and the mobile phase consisted in a mixture  
of acetonitrile/ultra-pure water (70/30, v/v). The flow rate was set at 0.4 mL min<sup>-1</sup> and 50 μL  
injection was considered. Detection was carried out at 195 nm.

109

### 110 3. RESULTS AND DISCUSSIONS

111 **3.1. Effect of pH on the electroreduction of alachlor.** Alachlor **1** (Scheme 1), a common  
112 chloroacetanilide herbicide, was first analyzed on Bi electrode by cyclic voltammetry in  
113 different pH media (Figure 2).

114



115

Alachlor 1

Trichloroacetamide 2

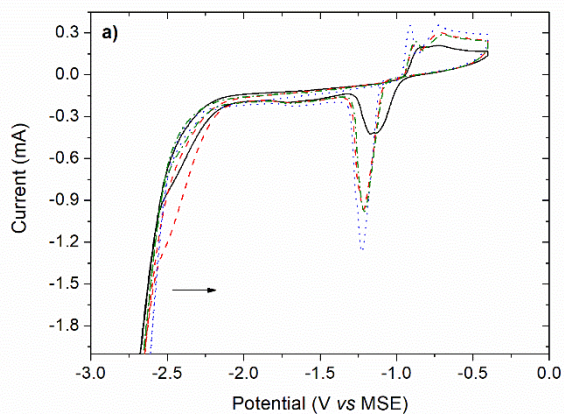
Pretilachlor 3

Dimethenamid 4

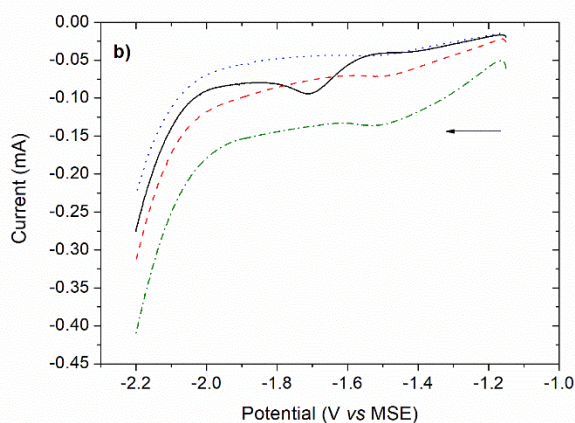
116 **Scheme 1.** Structure of chloroacetamide derivatives

117

118



119



120

121 **Figure 2.** Cyclic voltammetry analysis on a bismuth disk electrode (1.5 mm diameter) of a  
122 solution of 0.1 mol L<sup>-1</sup> Na<sub>2</sub>SO<sub>4</sub> at pH 3 (—), pH 7 (---), pH 10 (-.-.-), pH 13 (.....) (pH

123 adjusted with H<sub>2</sub>SO<sub>4</sub> or NaOH) without (a) and with (b) alachlor (200 ppm, 0.74 mmol L<sup>-1</sup>).

124 Scan rate: 0.1 V s<sup>-1</sup>.

125

126 A blank was first performed at different pH (Figure 2a). Oxidation peaks were observed around

127 -0.8- -0.4 V<sub>MSE</sub> on all cyclic voltammograms with a reduction peak at -1- -1.2 V<sub>MSE</sub> depending

128 on the pH. It corresponds to the formation of a layer of Bi salts on the electrode surface at

129 potentials less negative than -0.8 V<sub>MSE</sub> and their subsequent reduction.<sup>32-34</sup> In the presence of

130 alachlor, a peak can be observed for the four studied pH in the potential range from -1.5 to -1.7

131 V<sub>MSE</sub>, corresponding to the reduction of alachlor on bismuth. Compared with the reduction peak

132 of alachlor observed on glassy carbon electrode (Figure S1), the potentials are positively shifted

133 for all studied pH (Table 1). Interestingly, the difference of potential increased with the pH of

134 the solution from 270 to 510 mV, suggesting a more efficient catalysis for pH ≥ 7.

135

136 **Table 1.** Peak potential of studied compounds in 0.1 M Na<sub>2</sub>SO<sub>4</sub> on Bi and GC electrodes and

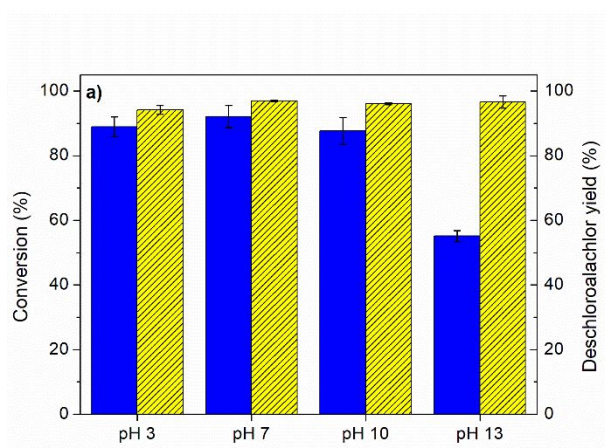
137 electron transfer coefficient calculated from cyclic voltammetry experiments

Chlorinated compounds		Peak potential (V <sub>MSE</sub> )		ΔE <sub>(Bi-GC)</sub> (V <sub>MSE</sub> )	α
		GC	Bi		
Alachlor	pH 3	-1.98	-1.71	0.27	0.34
	pH 7	-1.91	-1.50	0.41	0.18
	pH 10.5	-2.01	-1.52	0.49	0.08
	pH 13	-2.04	-1.53	0.51	0.18
Chloroacetamide		-2.22	-1.89	0.33	--
Dichloroacetamide		-2.16	-1.88	0.28	--
		-1.83	-1.41	0.42	--
Trichloroacetamide		-2.16	-1.91	0.25	0.32
		-1.87	-1.49	0.38	0.16
		-1.39	-1.12	0.27	0.50
Pretilachlor		-1.84	-1.62	0.22	0.21
Dimethenamid		-1.95	-1.68	0.27	0.25
Trichloroacetic acid		--	-2.02	--	--
		-2.02	-1.29	0.73	0.31
Allyl chloride		-1.96	-1.64	0.32	0.32
Chloroacetic acid		--	--	--	--

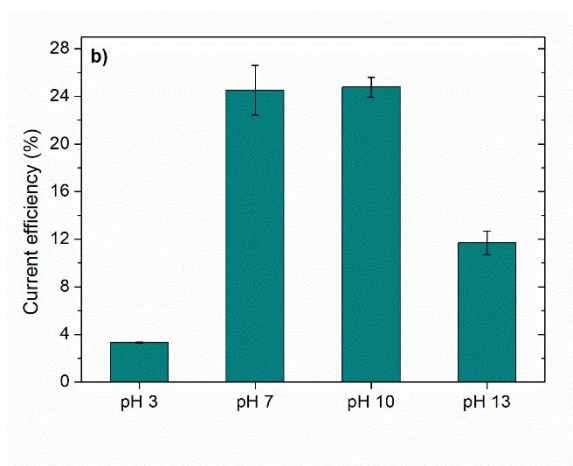
138



139 Electroreduction of a solution of 50 ppm ( $0.18 \text{ mol L}^{-1}$ ) alachlor in  $0.05 \text{ mol L}^{-1} \text{ Na}_2\text{SO}_4$  were  
140 performed at different pH at a potential of  $-1.8 \text{ V}_{\text{MSE}}$  (Figure 3a). The reaction was very efficient  
141 in all media with a conversion of alachlor around 96%. The yield of its dechlorinated derivative,  
142 deschloroalachlor, was estimated by UPLC-MS/MS to be around 90% for electrolyses  
143 performed at pH 3, 7 and 10, showing the high selectivity of the dehalogenation process. Indeed,  
144 previous reductive dehalogenation of alachlor performed on Ni-coated graphite felt modified  
145 by silver nanoparticles led to the formation of deschloralachlor with a yield around 76%,  
146 underlining the high selectivity of bismuth.<sup>35</sup>



147



148

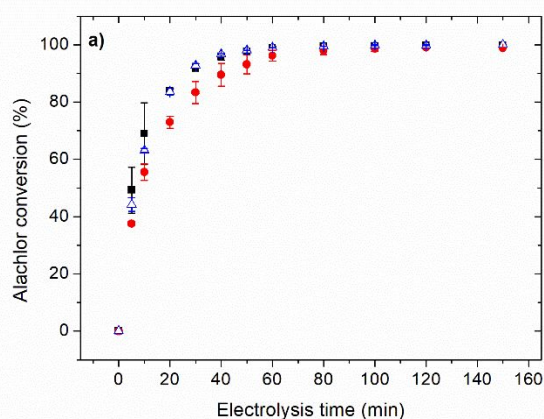
149 **Figure 3.** a) conversion yield of alachlor (hatched yellow area) and yield of deschloroalachlor  
150 (blue area) after 1 h of electrolysis at  $-1.8 \text{ V}_{\text{MSE}}$  of 50 ppm ( $0.18 \text{ mol L}^{-1}$ ) alachlor in  $0.05 \text{ mol}$   
151  $\text{L}^{-1} \text{ Na}_2\text{SO}_4$  (pH adjusted with  $\text{H}_2\text{SO}_4$  or  $\text{NaOH}$ ) for 1 h b) current efficiency after electrolysis.  
152 Error bars are based on two experiments.

153

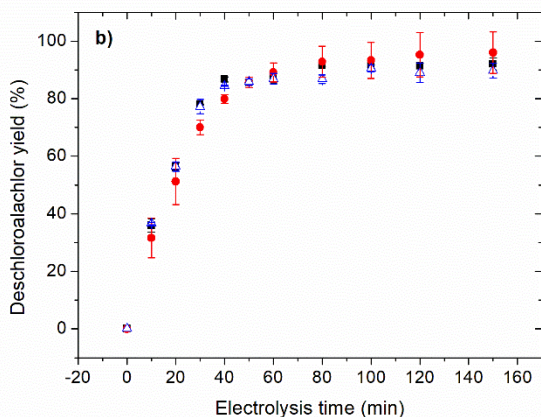
154 The low yield of deschloroalachlor at pH 13 showed thatalachlor underwent other reduction  
155 processes than dechlorination and that the reaction was less selective, even if no other peak than  
156 those of deschloroalachlor was observed in HPLC even after 5h of electrolysis. The current  
157 efficiency was calculated according to the amount of chloride ions measured by ion  
158 chromatography (Figure 3b). The highest current efficiencies were obtained at pH 7 and 10.  
159 The low value obtained at pH 3 is probably due to the competition with hydrogen evolution  
160 since the reduction ofalachlor occurred at a potential ( $-1.7 V_{MSE}$ ) closed to the reduction of  
161 water. The lower current efficiency observed at pH 13 is in accordance with the presence of  
162 side reactions that led to the formation of chlorinated by-products.

163

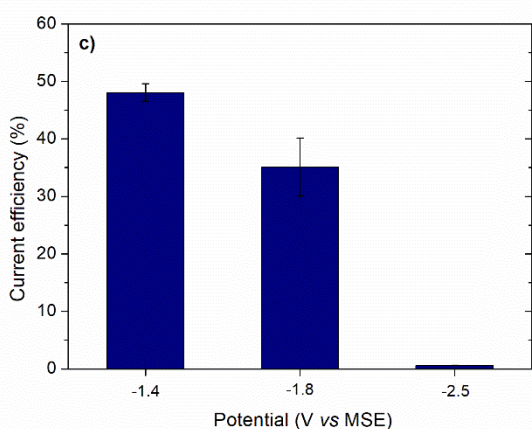
164 **3.2. Effect of the applied potential on the electroreduction ofalachlor.** Sincealachlor  
165 dechlorination was very effective and selective at pH 7, this medium was considered thereafter.  
166 Reductive dechlorination ofalachlor was then tested at three different applied potentials to  
167 check the effect on the selectivity of the reaction and on its current efficiency (Figure 4).  
168 Alalachlor conversion was almost total for all applied potentials after 80 min of electrolysis,  
169 although the kinetic was slightly slower at  $-1.4 V_{MSE}$ .



170



171



172

173

174 **Figure 4.** a) alachlor conversion, b) yield of deschloroalachlor c) current efficiency after the  
175 electrolysis of 50 ppm alachlor in 0.05 mol L<sup>-1</sup> Na<sub>2</sub>SO<sub>4</sub> (pH 7) at potentials of -1.4 V<sub>MSE</sub> (●), -  
176 1.8 V<sub>MSE</sub> (■) and -2.5 V<sub>MSE</sub> (▲). Error bars are based on two experiments.

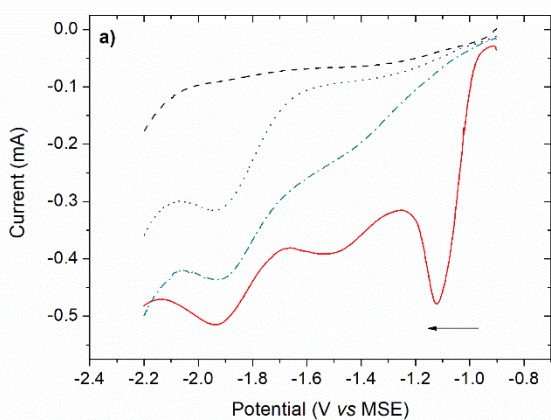
177

178 The selectivity toward the formation of deschloroalachlor was also very high for all studied  
179 potentials, leading to a yield of 89-96% (Figure 4b). The effect of the applied potential on the  
180 current efficiency was significant. It decreased for more negative potentials, owing to the  
181 competition with hydrogen evolution, and reached a value of 48 ± 2% for electroreduction  
182 performed at -1.4 V<sub>MSE</sub>.

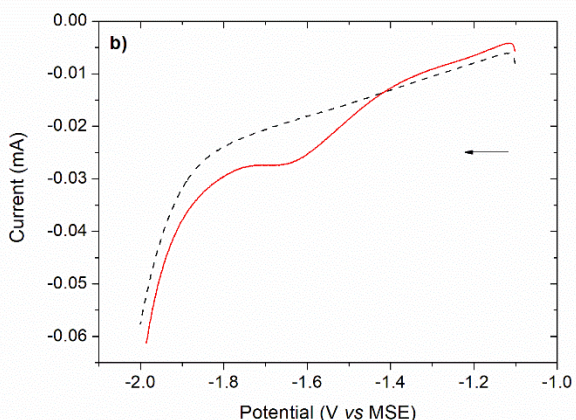
183 Comparison with results previously reported for the reductive dechlorination of alachlor on Ni-  
184 coated graphite felt modified with silver nanoparticles (96% conversion for 100 min electrolysis  
185 with a current efficiency up to 33%<sup>35</sup>) underlines the high catalytic efficiency of bismuth.  
186 Furthermore, the high selectivity of the reaction on bismuth is noteworthy. Deschloroalachlor  
187 yield reached 96%, against 76% on Ni-coated graphite felt modified with silver nanoparticles<sup>35</sup>  
188 and 86% with a Co catalyst.<sup>27-28</sup>

189

190 **3.3. Electroreduction of other chloroacetamides.** To confirm the high catalytic activity of  
191 bismuth toward the electroreduction of chloroacetamide pollutants, the reductive  
192 dechlorinations of trichloroacetamide, a disinfection by-product, and, pretilachlor and  
193 dimethenamid, two herbicides, were investigated. The electrocatalytic activity of bismuth was  
194 first studied by cyclic voltammetry (Figure 5).

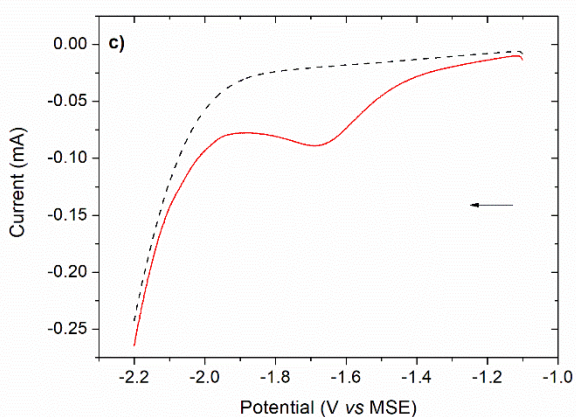


195



196

197



198

199 **Figure 5.** Cyclic voltammogram of a solution of  $0.1 \text{ mol L}^{-1} \text{ Na}_2\text{SO}_4$  at pH 7 on a bismuth disk  
200 electrode ( $\text{Ø } 5\text{mm}$ ) (-----) a)  $20 \text{ mmol L}^{-1}$  trichloroacetamide (—), dichloroacetamide (-.-.-),  
201 chloroacetamide (. . . . .) b)  $1 \text{ mmol L}^{-1}$  pretilachlor c)  $3.6 \text{ mmol L}^{-1}$  dimethenamid. Scan rate:  
202  $0.1 \text{ V s}^{-1}$ .

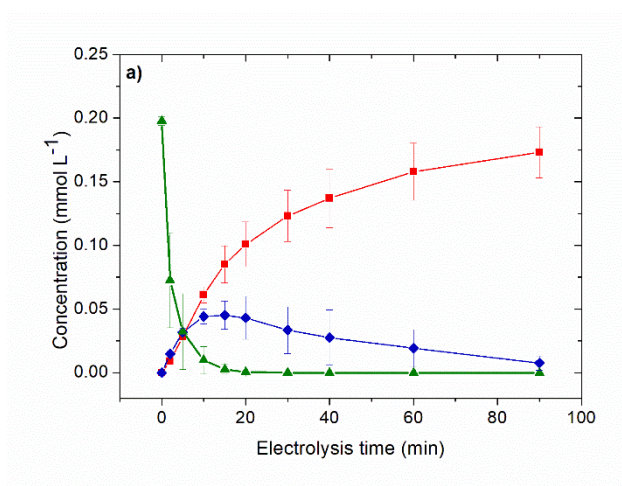
203

204 Trichloroacetamide exhibited three reduction peaks at  $-1.1$ ,  $-1.5$  and  $-1.9 \text{ V}_{\text{MSE}}$ . Comparison  
205 with the voltammograms of di and chloroacetamides showed that they correspond to the  
206 reduction of each C-Cl bond, the first one being the easiest to reduce. The reduction of the two  
207 first C-Cl bonds happened on glassy carbon electrode with a negative shift of potential of  $0.25$   
208 to  $0.38 \text{ V}$  (Figure S2, Table 1). This difference of potential underlines the high catalytic activity

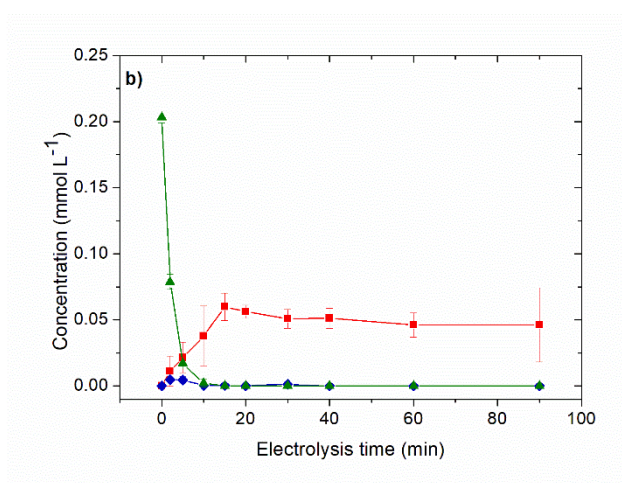
209 of bismuth toward the reduction of these chloroacetamide compounds compared with glassy  
210 carbon. Pretilachlor and dimethenamid were also reduced at  $-1.6$  and  $-1.7$   $V_{MSE}$ , respectively  
211 (Figure 5b and c). Their reduction on glassy carbon electrode occurred at more negative  
212 potentials with a shift of  $0.22$  and  $0.27$  V, respectively (Figure S3, Table 1), highlighting the  
213 high catalytic activity of bismuth for these species.

214 Bulk electrolyses of trichloroacetamide were performed at  $-1.2$ ,  $-1.6$  and  $-2$   $V_{MSE}$  in  $0.05$  mol  
215  $L^{-1}$   $Na_2SO_4$  at pH 7 (Figure 6).

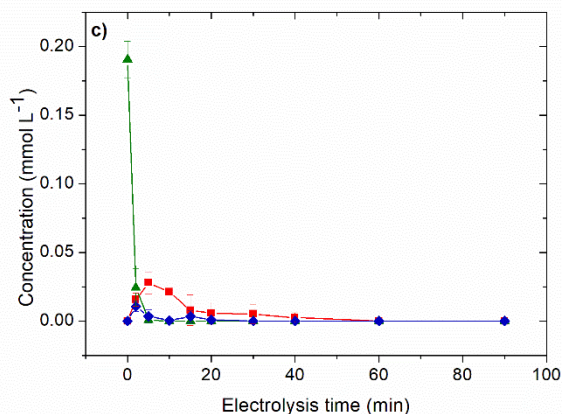
216



217



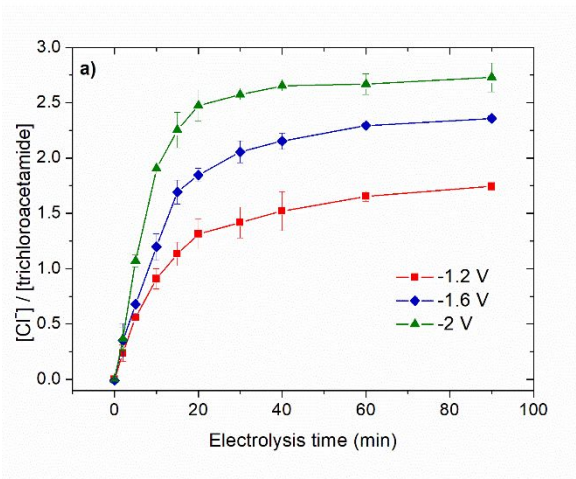
218



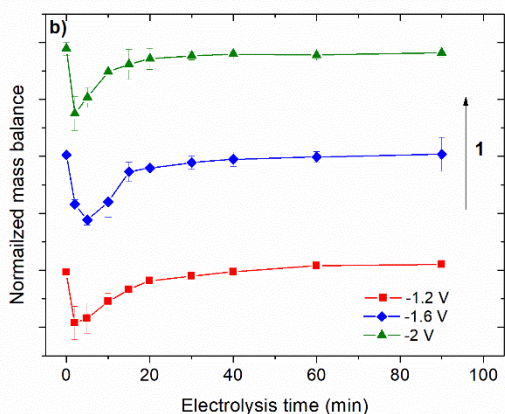
219

220 **Figure 6.** Concentrations of trichloroacetamide (-▲-), dichloroacetamide (-◆-) and  
221 chloroacetamide (-■-) during electrolysis of 0.2 mmol L<sup>-1</sup> trichloroacetamide in 0.05 mol L<sup>-1</sup>  
222 Na<sub>2</sub>SO<sub>4</sub> at potential of a) -1.2 V<sub>MSE</sub>, b) -1.6 V<sub>MSE</sub> and c) -2.0 V<sub>MSE</sub> with initial pH 7. Error bars  
223 are based on at least two experiments.

224 The concentration of chloride ions was measured by ion chromatography (Figure 7a).



225



226

227 **Figure 7.** a) Chloride ions concentration and b) Mass balance of chlorinated species based on  
228 trichloroacetamide, dichloroacetamide, chloroacetamide and chloride ions normalized by the  
229 initial concentration of trichloroacetamide for electrolyses performed at -1.2, -1.6 and -2  $V_{MSE}$   
230 in  $0.05 \text{ mol L}^{-1} \text{ Na}_2\text{SO}_4$  at pH 7. Error bars are based on at least two experiments.

231

232 When the electrolysis was performed at -1.2  $V_{MSE}$ , the formation of dichloroacetamide was not  
233 selective and the presence of chloroacetamide was also observed. The concentration of chloride  
234 ions was 1.5 times the initial concentration of trichloroacetamide (Figure 7a) after 90 min  
235 electrolysis whereas the total reduction of trichloroacetamide and dichloroacetamide as  
236 observed in Figure 6a should lead to a ratio of 2. This result shows that the reduction of  
237 trichloroacetamide and dichloroacetamide led to other by-products than their dechlorinated  
238 derivatives. This was confirmed by the presence of new peaks in HPLC analyses (Figure S4).  
239 Mass balance of chloride atoms calculated from the amount of chloride ions and remaining  
240 dichloroacetamide and chloroacetamide also indicated the formation of other chlorinated by-  
241 products in the first 20 min of electrolysis (Figure 7b). After 90 min electrolysis, the ratio  
242 reached a value of 1 for electrolyses performed at -1.2 and -1.6 V, showing that a total  
243 dechlorination of these by-products occurred. Thus the only chlorinated compounds remaining  
244 in solution after electrolyses performed at -1.2 and -1.6 V were chloroacetamide and chloride



245 ions. For reduction performed at -2 V, a ratio of 0.9 was reached indicating the presence of a  
 246 few unidentified chlorinated by-products after 90 min electrolysis. This was confirmed by the  
 247 results highlighted in Figure 6c showing that trichloroacetamide, dichloroacetamide and  
 248 monochloroacetamide were totally reduced after 90 min electrolysis although the ratio of  
 249 chloride ions was only 2.7 (Figure 7a). Current efficiencies after 30 min of bulk electrolysis are  
 250 given in Table 2. The dechlorination yield increased when a more negative potential was used.  
 251 However, potentials more negative than -1.6 V also led to a decrease of the current efficiency  
 252 owing to competition with hydrogen evolution.

253 **Table 2.** Dechlorination yield and current efficiency of 0.2 mmol L<sup>-1</sup> chloroacetamide  
 254 electroreduction on the Bi modified electrode after 30 min electrolysis in 0.05 mol L<sup>-1</sup> Na<sub>2</sub>SO<sub>4</sub>  
 255 at pH 7.

Pollutant	Applied potential (V <sub>MSE</sub> )	Cl <sup>-</sup> yield (%) <sup>a</sup>	Current efficiency (%)
Trichloroacetamide	-1.2	47 ± 5	50 ± 4
	-1.6	69 ± 3	58 ± 7
	-1.8	72 ± 5	28.84 ± 0.04
	-2.0	85.7 ± 0.1	14 ± 4
Dichloroacetamide	-1.2	26 ± 1	20 ± 4
	-1.6	60 ± 7	47 ± 12
	-1.8	72 ± 1	21.6 ± 0.1
	-2.0	89 ± 3	11 ± 2
Chloroacetamide	-1.6	32 ± 2	15.4 ± 0.8
	-1.8	76.4 ± 0.5	12.0 ± 0.1
	-2.0	95.1 ± 7	6.2 ± 0.6

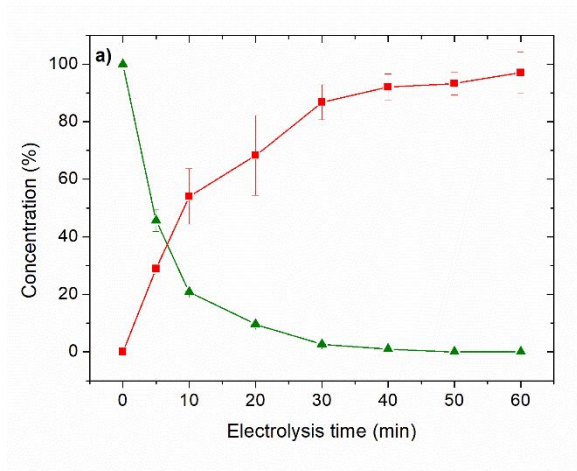
256 <sup>a</sup> The Cl<sup>-</sup> yield is calculated from the initial amount of pollutant

257

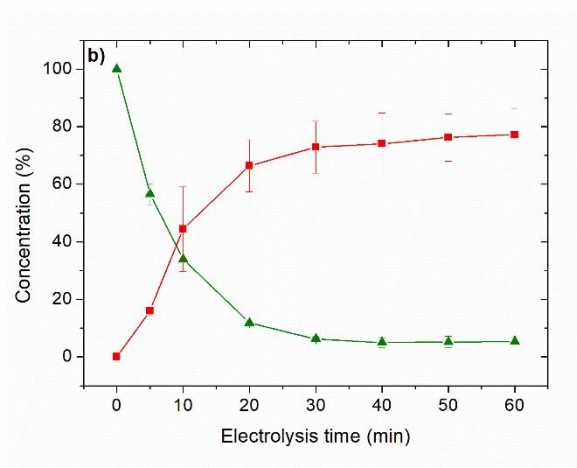
258 The same experiments were carried out with dichloroacetamide and chloroacetamide for  
 259 comparison (Figure S5 to S8). Electrolyses performed at less negative potentials led to higher  
 260 current efficiency since the competition with hydrogen evolution decreased. However, higher  
 261 electrolysis time would be required to obtain good dechlorination yields. Mass balance of  
 262 chloride ions showed the formation of chlorinated by-products at the beginning of the

263 electrolyses, especially for electrolyses performed at -2 V (Figure S6 and S8). However, the  
264 variation of the mass balance is less important than for the reduction of trichloroacetamide,  
265 showing that the reduction is more selective toward the formation of acetamide.

266 Bulk electrolyses of 0.2 mmol L<sup>-1</sup> pretilachlor and dimethenamid were performed at -1.8 V<sub>MSE</sub>  
267 in 0.05 mol L<sup>-1</sup> Na<sub>2</sub>SO<sub>4</sub> at pH 7. The pollutants were totally reduced after 60 min of electrolysis  
268 (Figure 8a and b).



269



270

271 **Figure 8.** Concentration of chlorinated starting material (-▲-) and dechlorination yield (-■-)   
272 during electroreduction of 0.2 mmol L<sup>-1</sup> a) pretilachlor and b) dimethenamid in 0.05 mol L<sup>-1</sup>   
273 Na<sub>2</sub>SO<sub>4</sub> at potential of -1.8 V<sub>MSE</sub> with initial pH 7. Error bars are based on at least two   
274 experiments.

275

276 The dechlorination yields estimated by measuring the concentration of chloride ions by ion  
 277 chromatography were 97% and 77% for pretilachlor and dimethenamid, respectively,  
 278 underlining the good efficiency of the dechlorination process.

279 A comparison of the dechlorination yields and current efficiencies after 30 min electrolysis for  
 280 the studied chloroacetamide compounds is given in Table 3.

281

282 **Table 3.** Dechlorination yield and current efficiency after 30 min of electroreduction at -1.8  
 283  $V_{MSE}$  of 0.2 mmol L<sup>-1</sup> chlorinated compounds on the Bi modified electrode in 0.05 mol L<sup>-1</sup>  
 284 Na<sub>2</sub>SO<sub>4</sub> at pH 7.

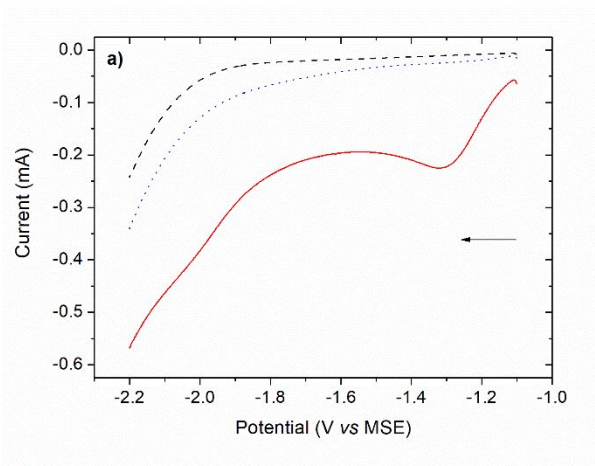
Pollutant	Cl <sup>-</sup> Yield (%)	Current efficiency (%)
Pretilachlor	97 ± 7	20 ± 2
Alachlor	85.2 ± 0.3	26 ± 3
Dimethenamid	77 ± 9	11.8 ± 0.4
Chloroacetamide	76.4 ± 0.5	12.0 ± 0.1
Dichloroacetamide	72 ± 1	21.6 ± 0.1
Trichloroacetamide	72 ± 5	28.84 ± 0.04
Trichloroacetic acid	35.5 ± 2	19.0 ± 0.1
Allyl chloride	39.3 ± 0.6	5.61 ± 0.06
Chloroacetic acid	0	--

285

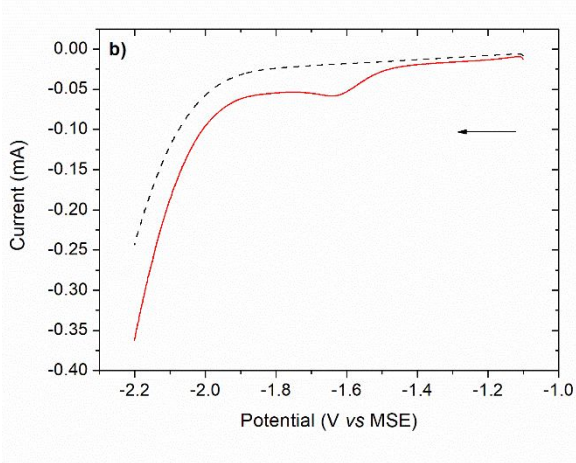
286 The kinetic of the reaction clearly depends on the chemical structure of the pollutants with  
 287 higher dechlorination yields for chloroacetanilide derivatives (pretilachlor and alachlor).  
 288 Current efficiencies were around 10-20% owing to competition with hydrogen evolution at -  
 289 1.8  $V_{MSE}$ . The electroreduction on bismuth of chloroacetamides is so very efficient with a total  
 290 reduction of the targeted compounds and high dechlorination yields (between 72 and 97%) after  
 291 30 min electrolysis.

292

293 **3.4. Electroreduction of other compounds with activated carbon atoms.** The ability of  
294 bismuth to reduce other compounds with activated carbon atoms was also tested with  
295 trichloroacetic acid, chloroacetic acid and allyl chloride. Cyclic voltammetry analyses (Figure  
296 9a) revealed two reduction peaks at -1.29 and -2.02 V<sub>MSE</sub> for trichloroacetic acid. Whereas the  
297 first reduction occurred at a potential close to those of trichloroacetamide, the second one was  
298 at a more negative potential and the analysis of chloroacetic acid did not reveal the presence of  
299 a peak.



300



301

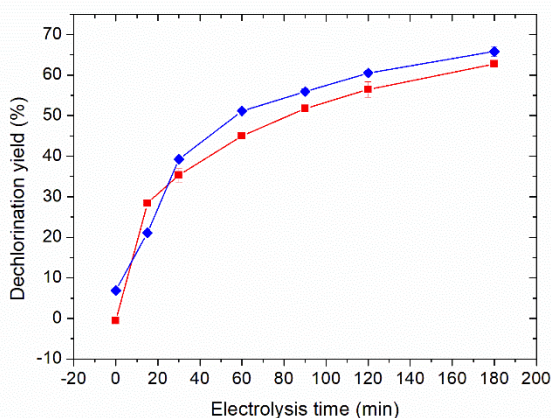
302 **Figure 9.** Cyclic voltammogram of a solution of 0.1 mol L<sup>-1</sup> Na<sub>2</sub>SO<sub>4</sub> at pH 7 on a bismuth disk  
303 electrode (Ø 5mm) (-----) of a) 20 mmol L<sup>-1</sup> trichloroacetic acid (—), 20 mmol L<sup>-1</sup> chloroacetic  
304 acid (.....) b) 20 mmol L<sup>-1</sup> allyl chloride. Scan rate: 0.1 V s<sup>-1</sup>.

305

306 However, compared with the reduction peak of trichloroacetic acid observed on glassy carbon  
307 electrode (Table 1, Figure S9), the first reduction peak was positively shifted by 0.73 V and the  
308 second reduction was not observed on glassy carbon, underlining the high catalytic ability of  
309 bismuth to reduce trichloroacetic acid. As seen in Figure 9b, the reduction of allyl chloride  
310 occurred at -1.64 V, i.e. 0.32 V earlier than on glassy carbon (Table 1, Figure S9), confirming  
311 also the catalytic effect of bismuth.

312 Bulk electrolyses of 0.2 mmol L<sup>-1</sup> trichloroacetic acid, chloroacetic acid and allyl chloride were  
313 then carried out at -1.8 V<sub>MSE</sub> in 0.05 mol L<sup>-1</sup> Na<sub>2</sub>SO<sub>4</sub> at pH 7.

314 The reduction of trichloroacetic acid led to a dechlorination yield of 63% after 180 min  
315 electrolysis (Figure 10).



316

317 **Figure 10.** Dechlorination yield during electroreduction of 0.2 mmol L<sup>-1</sup> trichloroacetic acid (-  
318 ■-) and allyl chloride (-♦-) in 0.05 mol L<sup>-1</sup> Na<sub>2</sub>SO<sub>4</sub> at potential of -1.8 V<sub>MSE</sub> with initial pH 7.  
319 Error bars are based on two ion chromatography analyses.

320

321 The same experiment performed at -2 V<sub>MSE</sub> gave a dechlorination yield of 66% after 4h,  
322 showing that only two chloride atoms can be removed from trichloroacetic acid in these  
323 conditions. Thus these results confirmed cyclic voltammetry analyses that showed the presence

324 of only two reduction waves. Moreover, the electroreduction of chloroacetic acid performed at  
325  $-1.8 V_{MSE}$  failed in these conditions. The lowest reactivity of trichloroacetic acid compared with  
326 trichloroacetamide can be explained by the presence of a carboxylate group at pH 7 instead of  
327 an electron withdrawing amide group.

328 Allyl chloride was dechlorinated with a yield of 66% after 180 min electrolysis. The reaction  
329 was clearly slower than with  $\alpha$ -halocarbonyl compounds.

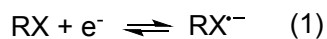
330 A comparison of electroreductions performed at  $-1.8 V_{MSE}$  for 30 min on bismuth electrode is  
331 made in Table 3. The highest dechlorination yields were obtained for chloroacetamide  
332 compounds, especially chloroacetanilides. The reductions of other studied chlorinated  
333 compounds containing an activated carbon atom were slower even if the difference in peak  
334 potentials between bismuth and glassy carbon electrodes observed in cyclic voltammetry (Table  
335 1) was in the same order of magnitude. The reduction of chlorinated compounds on Bi appears  
336 to be specific to species with an activated carbon atom since our attempts to reduce other  
337 derivatives such as chloroaromatic compounds failed.

338

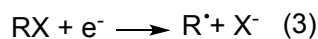
339 **3.5. Mechanism.** Additional insights about the mechanism were derived from the cyclic  
340 voltammetry studies notably the variations of the peak potential  $E_p$  as a function of the scan  
341 rates. These variations have been demonstrated to be a good criterion to distinguish between  
342 different mechanisms.<sup>36</sup>  $E_p$  was found to linearly vary with  $\log(\nu)$  with slopes in the range of  
343  $-43$  -  $-380$  mV/ $\log(\nu)$  (Figure S9 to S13). Such large slopes are indicative of a control of the  
344 electrochemical process by the electron transfer that could (or not) be associated with a  
345 chemical step. A control by the electron transfer is indicative of large reorganisation energy  
346 upon the electron transfer. As discussed previously, the electrochemical reduction of a carbon-  
347 halogen bond could be described as involving a chemical step with the electron transfer that

348 globally could occur *via* a dissociative electron transfer, according to a stepwise or a concerted  
 349 mechanism (Scheme 2):

Stepwise mechanism



Concerted mechanism



351 **Scheme 2.** Stepwise and concerted mechanisms for the reduction of a carbon-halogen bond

352 For a concerted mechanism, the heterogeneous electron transfer contains the additional  
 353 contribution of the dissociative energy of the halogen-bond, which is not the case for a stepwise  
 354 mechanism. Thus, a control by the electron transfer falls in line with a concerted mechanism.  
 355 The slope of the variation of  $E_p$  with  $\log(v)$  is equal to  $1.151 RT/\alpha F^{37-38}$  where  $\alpha$  is the charge  
 356 transfer coefficient,  $T$  the temperature,  $R$  the gas constant,  $F$  the Faraday constant. Using this  
 357 relation, the charge transfer coefficient  $\alpha$  was calculated for all studied molecules (Table 1). In  
 358 the framework of the Marcus-Hush model,  $\alpha$  depends on the free energy  $\Delta G^\circ$  of the reaction  
 359 *i.e.* the difference between  $E_p$  and the thermodynamic potential (Equation 5).<sup>39</sup>

360

361 
$$\alpha = \frac{\partial \Delta G_f^\ddagger}{\partial \Delta G^\circ} = 0.5 \left( 1 + \frac{\Delta G^\circ}{4 \Delta G_0^\ddagger} \right) \quad (5)$$

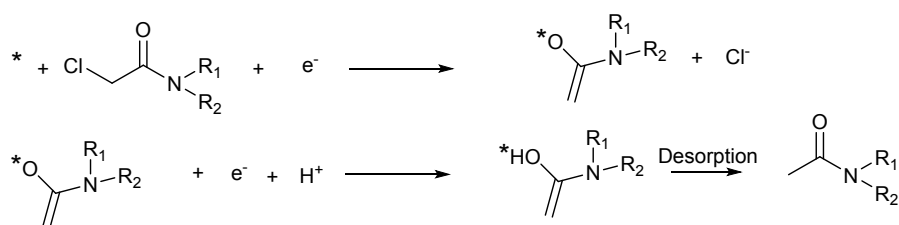
362 with  $\Delta G_f^\ddagger$  the forward activation free energy,  $\Delta G^\circ$  the standard free energy of reaction,  $\Delta G_0^\ddagger$   
 363 the standard activation free energy (intrinsic barrier).

364

365 A small value of  $\alpha$  is thus indicative of a large overpotential and likely of concerted mechanism  
 366 as found for the electroreduction of alkyl halide.<sup>36</sup> For all considered molecules,  $\alpha$  was found

367 to be much smaller than  $\leq 0.5$  that indeed supports the occurrence of a concerted electron  
 368 transfer with the chemical steps.

369 In the case of  $\alpha$ -halocarbonyl derivatives, it was shown that adsorbates with O–Bi bonds are  
 370 systematically more stable than those with C–Bi bonds.<sup>40-41</sup> For example, \*OCHO is  $-0.87$  eV  
 371 more stable than \*COOH. The high affinity of bismuth for the oxygen atom could explain the  
 372 observed high catalytic activity toward the reduction of chloroacetamide compounds and  
 373 trichloroacetic acid. Based on these considerations, we could propose the following mechanism  
 374 (Scheme 3) for the electroreduction of chloroacetamide on Bi :



375

376

377 **Scheme 3.** Electroreduction of chloroacetamide compounds on bismuth.

378

379 For  $\alpha$ -haloallyl derivatives such as allyl chloride, it can be deduced that the Bi ability to catalyse  
 380 their reduction is due to an interaction between bismuth and the double bond although this  
 381 interaction is probably lower as suggested by the slower kinetic observed for the dechlorination  
 382 process.

383 In conclusion, this work demonstrates for the first time the electrocatalytic activity of bismuth  
 384 to break the carbon-halogen bond. Chloroacetanilide herbicides such as alachlor and  
 385 pretilachlor can be totally reduced with a high selectivity, leading to dechlorination yields  
 386 higher than 96%. The high catalytic activity of bismuth toward the reduction of other  
 387 chloroacetamides pollutants has also been shown. Interestingly, the electroreduction process is  
 388 efficient on all compounds containing an activated carbon atom as it has been demonstrated in



389 this work with  $\alpha$ -halocarbonyl and  $\alpha$ -haloallyl derivatives. Cyclic voltammetry experiments  
390 show that the electrochemical reduction of the carbon-halogen bond implies a dissociative  
391 electron transfer *via* a concerted mechanism. Therefore, the high affinity of bismuth for oxygen  
392 atoms is probably responsible for its high catalytic ability toward the reduction of  $\alpha$ -  
393 halocarbonyl compounds. This cost-effective and green porous bismuth electrode incorporated  
394 in a flow electrochemical system would be particularly interesting for the water treatment of  
395 biorecalcitrant pollutants. A coupling with a biological treatment is possible if the dechlorinated  
396 compounds are biodegradable. If the by-products are still persistent, a coupling process with  
397 electro-Fenton can be advantageously envisaged as it has been previously demonstrated with  
398 alachlor.<sup>42</sup>

399

#### 400 **ACKNOWLEDGEMENTS**

401 Y. Y. Lou thanks the China Scholarship Council for a Ph. D. grant.

402

#### 403 **Supporting Information.**

404 Comparison of electroreduction on Bi and glassy carbon electrodes by linear sweep  
405 voltammetry analysis (Figures S1 to S3 and S9), HPLC analysis during electroreduction of  
406 trichloroacetamide (Figure S4), electroreduction of dichloroacetamide and chloroacetamide  
407 (Figures S5 to S8), linear sweep voltammetry analyses for mechanistic investigations (Figure  
408 S10 to S13).

409

#### 410 **REFERENCES**

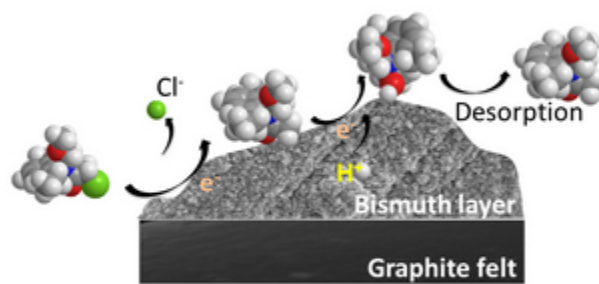
- 411 (1) Liu, X.; Xiao, M.; Xu, L.; Miao, Y.; Ouyang, R. Characteristics, applications and  
412 determination of bismuth. *J. Nanosci. Nanotechnol.* **2016**, *16*, 6679-6689.
- 413 (2) Ollevier, T. New trends in bismuth-catalyzed synthetic transformations. *Org. Biomol.*  
414 *Chem.* **2013**, *11*, 2740-2755.
- 415 (3) Bothwell, J. M.; Krabbe, S. W.; Mohan, R. S. Applications of bismuth(III) compounds  
416 in organic synthesis. *Chem. Soc. Rev.* **2011**, *40*, 4649-4707.
- 417 (4) Shen, Z.; Zhang, J.; Zou, H.; Yang, M. A novel one-pot Reformatskii type reaction via  
418 bismuth salt in aqueous media. *Tetrahedron Lett.* **1997**, *38*, 2733-2736.
- 419 (5) Ren, P.-D.; Pan, S.-F.; Dong, T.-W.; Wu, S.-H. Selective reduction of  $\alpha,\beta$ -unsaturated  
420 esters with NaBH<sub>4</sub>-BiCl<sub>3</sub> system. *Synth. Commun.* **1995**, *25*, 3395-3399.
- 421 (6) Lee, Y. J.; Chan, T. H. Bismuth-mediated reductive dehalogenation of  $\alpha$ -halocarbonyl  
422 compounds. *Can. J. Chem.* **2004**, *82*, 71-74.
- 423 (7) Hasiotis, C.; Kokkinidis, G. Use of platinum/metal(underpotential deposited) (metal =  
424 lead, thallium, bismuth) modified electrodes to the catalytic electroreduction of heterocyclic  
425 nitro compounds. II. 2-Nitro and 4-nitroimidazole. *Electrochim. Acta* **1992**, *37*, 1231-1237.
- 426 (8) Kokkinidis, G.; Hasiotis, K.; Sazou, D. Use of platinum/metal(underpotential  
427 deposited) (metal=lead, thallium, bismuth) modified electrodes to the catalytic electroreduction  
428 of heterocyclic nitro compounds. I. 3-Nitro-1H-1,2,4-triazole. *Electrochim. Acta* **1990**, *35*,  
429 1957-1964.
- 430 (9) Kokkinidis, G.; Papanastasiou, G. Electrocatalytic reduction of 4-nitropyridine- N-  
431 oxide on platinum/M (UPD) modified electrodes in aqueous acid solutions. *Electrochim. Acta*  
432 **1989**, *34*, 803-809.
- 433 (10) Sayed, S. M.; Juettner, K. Electrocatalysis of oxygen and hydrogen peroxide reduction  
434 by UPD of bismuth on poly- and monocrystalline gold electrodes in acid solutions. *Electrochim.*  
435 *Acta* **1983**, *28*, 1635-1641.

- 436 (11) Chen, C. H.; Gewirth, A. A. Correlation of electrode surface structure with activity  
437 toward peroxide electroreduction for bismuth monolayers on gold(111). *J. Am. Chem. Soc.*  
438 **1992**, *114*, 5439-5440.
- 439 (12) Li, X.; Gewirth, A. A. Oxygen Electroreduction through a Superoxide Intermediate on  
440 Bi-Modified Au Surfaces. *J. Am. Chem. Soc.* **2005**, *127*, 5252-5260.
- 441 (13) Kwon, Y.; Birdja, Y. Y.; Raoufmoghaddam, S.; Koper, M. T. M. Electrocatalytic  
442 Hydrogenation of 5-Hydroxymethylfurfural in Acidic Solution. *ChemSusChem* **2015**, *8*, 1745-  
443 1751.
- 444 (14) Kwon, Y.; de Jong, E.; Raoufmoghaddam, S.; Koper, M. T. M. Electrocatalytic  
445 Hydrogenation of 5-Hydroxymethylfurfural in the Absence and Presence of Glucose.  
446 *ChemSusChem* **2013**, *6*, 1659-1667.
- 447 (15) Kwon, Y.; Koper, M. T. M. Electrocatalytic Hydrogenation and Deoxygenation of  
448 Glucose on Solid Metal Electrodes. *ChemSusChem* **2013**, *6*, 455-462.
- 449 (16) DiMeglio, J. L.; Rosenthal, J. Selective Conversion of CO<sub>2</sub> to CO with High Efficiency  
450 Using an Inexpensive Bismuth-Based Electrocatalyst. *J. Am. Chem. Soc.* **2013**, *135*, 8798-8801.
- 451 (17) Medina-Ramos, J.; DiMeglio, J. L.; Rosenthal, J. Efficient reduction of CO<sub>2</sub> to CO  
452 with high current-density by using in-situ or ex-situ prepared Bi-based materials. *J. Am. Chem.*  
453 *Soc.* **2014**, *136*, 8361-8367.
- 454 (18) He, S.; Ni, F.; Ji, Y.; Wang, L.; Wen, Y.; Bai, H.; Liu, G.; Zhang, Y.; Li, Y.; Zhang, B.;  
455 Peng, H. The p-Orbital Delocalization of Main-Group Metals to Boost CO<sub>2</sub> Electroreduction.  
456 *Angew. Chem., Int. Ed.* **2018**, *57*, 16114-16119.
- 457 (19) Atifi, A.; Boyce, D. W.; Di Meglio, J. L.; Rosenthal, J. Directing the Outcome of CO<sub>2</sub>  
458 Reduction at Bismuth Cathodes Using Varied Ionic Liquid Promoters. *ACS Catal.* **2018**, *8*,  
459 2857-2863.

- 460 (20) Xu, Y.; Zhu, Y.; Zhao, F.; Ma, C.-a. Electrocatalytic reductive dehalogenation of  
461 polyhalogenated phenols in aqueous solution on Ag electrodes. *Applied Catalysis, A: General*  
462 **2007**, *324*, 83-86.
- 463 (21) Durante, C.; Isse, A. A.; Sandona, G.; Gennaro, A. Electrochemical  
464 hydrodehalogenation of polychloromethanes at silver and carbon electrodes. *Appl. Catal. B*  
465 *Environ.* **2009**, *88*, 479-489.
- 466 (22) Perini, L.; Durante, C.; Favaro, M.; Agnoli, S.; Granozzi, G.; Gennaro, A.  
467 Electrocatalysis at palladium nanoparticles: Effect of the support nitrogen doping on the  
468 catalytic activation of carbon halogen bond. *Appl. Catal. B Environ.* **2014**, *144*, 300-307.
- 469 (23) Simonet, J.; Jouikov, V. Gold and gold-graphene used as cathodic interfaces for scission  
470 of carbon-halogen bonds. Application to the building of anthraquinone-Au electrodes.  
471 *Electrochem. Commun.* **2014**, *40*, 58-62.
- 472 (24) Isse, A. A.; Huang, B.; Durante, C.; Gennaro, A. Electrocatalytic dechlorination of  
473 volatile organic compounds at a copper cathode. Part I: Polychloromethanes. *Appl. Catal. B*  
474 *Environ.* **2012**, *126*, 347-354.
- 475 (25) Durante, C.; Huang, B.; Isse, A. A.; Gennaro, A. Electrocatalytic dechlorination of  
476 volatile organic compounds at copper cathode. Part II: Polychloroethanes. *Appl. Catal. B*  
477 *Environ.* **2012**, *126*, 355-362.
- 478 (26) Verlato, E.; He, W.; Amrane, A.; Barison, S.; Floner, D.; Fourcade, F.; Geneste, F.;  
479 Musiani, M.; Seraglia, R. Preparation of Silver-Modified Nickel Foams by Galvanic  
480 Displacement and Their Use as Cathodes for the Reductive Dechlorination of Herbicides.  
481 *ChemElectroChem* **2016**, *3*, 2084-2092.
- 482 (27) He, W. Y.; Fontmorin, J. M.; Hapiot, P.; Soutrel, I.; Floner, D.; Fourcade, F.; Amrane,  
483 A.; Geneste, F. A new bipyridyl cobalt complex for reductive dechlorination of pesticides.  
484 *Electrochim. Acta* **2016**, *207*, 313-320.

- 485 (28) He, W.; Fontmorin, J.-M.; Soutrel, I.; Floner, D.; Fourcade, F.; Amrane, A.; Geneste, F.  
486 Reductive dechlorination of a chloroacetanilide herbicide in water by a Co complex-supported  
487 catalyst. *Mol. Catal.* **2017**, *432*, 8-14.
- 488 (29) He, W.; Lou, Y.; Verlato, E.; Soutrel, I.; Floner, D.; Fourcade, F.; Amrane, A.; Musiani,  
489 M.; Geneste, F. Reductive dehalogenation of a chloroacetanilide herbicide in a flow  
490 electrochemical cell fitted with Ag-modified Ni foams. *J. Chem. Technol. Biotechnol.* **2018**,  
491 *93*, 1572-1578.
- 492 (30) Abdallah, R.; Derghane, A.; Lou, Y.-Y.; Merdrignac-Conanec, O.; Floner, D.; Geneste,  
493 F. New porous bismuth electrode material with high surface area. *J. Electroanal. Chem.* **2019**,  
494 *839*, 32-38.
- 495 (31) Fontmorin, J. M.; He, W. Y.; Floner, D.; Fourcade, F.; Amrane, A.; Geneste, F.  
496 Reductive dehalogenation of 1,3-dichloropropane by a [Ni(tetramethylcyclam)]Br<sub>2</sub>-Nafion  
497 modified electrode. *Electrochim. Acta* **2014**, *137*, 511-517.
- 498 (32) Williams, D. E.; Wright, G. A. Nucleation and growth of anodic oxide films on bismuth.  
499 I. Cyclic voltammetry. *Electrochim. Acta* **1976**, *21*, 1009-1019.
- 500 (33) Vivier, V.; Regis, A.; Sagon, G.; Nedelec, J. Y.; Yu, L. T.; Cachet-Vivier, C. Cyclic  
501 voltammetry study of bismuth oxide Bi<sub>2</sub>O<sub>3</sub> powder by means of a cavity microelectrode  
502 coupled with Raman microspectrometry. *Electrochim. Acta* **2001**, *46*, 907-914.
- 503 (34) Li, W. S.; Long, X. M.; Yan, J. H.; Nan, J. M.; Chen, H. Y.; Wu, Y. M. Electrochemical  
504 behaviour of bismuth in sulfuric acid solution. *J. Power Sources* **2006**, *158*, 1096-1101.
- 505 (35) Lou, Y.-Y.; He, W.; Verlato, E.; Musiani, M.; Floner, D.; Fourcade, F.; Amrane, A.; Li,  
506 C.; Tian, Z.-Q.; Merdrignac-Conanec, O.; Coulon, N.; Geneste, F. Ni-coated graphite felt  
507 modified with Ag nanoparticles: a new electrode material for electro-reductive dechlorination.  
508 *J. Electroanal. Chem.* **2019**, *849*, 113357.

- 509 (36) Ammar, F.; Nadjo, L.; Saveant, J. M. Linear sweep voltammetry. Kinetic control by  
510 charge transfer and/or secondary chemical reactions. II. Reduction of carbonyl compounds. *J.*  
511 *Electroanal. Chem. Interfacial Electrochem.* **1973**, *48*, 146-149.
- 512 (37) Isse, A. A.; Gottardello, S.; Durante, C.; Gennaro, A. Dissociative electron transfer to  
513 organic chlorides: Electrocatalysis at metal cathodes. *Phys. Chem. Chem. Phys.* **2008**, *10*, 2409-  
514 2416.
- 515 (38) Bard, A. J.; Faulkner, L. R., *Electrochemical Methods: Fundamentals and Applications.*  
516 John Wiley & Sons, Inc: New York, 2001.
- 517 (39) Saveant, J.-M., *Elements of Molecular and Biomolecular Electrochemistry: An*  
518 *Electrochemical Approach to Electron Transfer Chemistry.* Wiley-Interscience: New Jersey,  
519 2006.
- 520 (40) Oh, W.; Rhee, C. K.; Han, J. W.; Shong, B. Atomic and Molecular Adsorption on the  
521 Bi(111) Surface: Insights into Catalytic CO<sub>2</sub> Reduction. *J. Phys. Chem. C* **2018**, *122*, 23084-  
522 23090.
- 523 (41) Koh, J. H.; Won, D. H.; Eom, T.; Kim, N.-K.; Jung, K. D.; Kim, H.; Hwang, Y. J.; Min,  
524 B. K. Facile CO<sub>2</sub> Electro-Reduction to Formate via Oxygen Bidentate Intermediate Stabilized  
525 by High-Index Planes of Bi Dendrite Catalyst. *ACS Catal.* **2017**, *7*, 5071-5077.
- 526 (42) Lou, Y.-Y.; Geneste, F.; Soutrel, I.; Amrane, A.; Fourcade, F. Alachlor dechlorination  
527 prior to an electro-Fenton process: Influence on the biodegradability of the treated solution.  
528 *Sep. Purif. Technol.* **2020**, *232*, 115936.
- 529



Graphical abstract

84x63mm (96 x 96 DPI)